



HAL
open science

Thermal aging of electrical cable insulation made of cross-linked low density polyethylene for under-hood application in automotive industry

Tetiana Salivon, Raphael Comte, Xavier Colin

► **To cite this version:**

Tetiana Salivon, Raphael Comte, Xavier Colin. Thermal aging of electrical cable insulation made of cross-linked low density polyethylene for under-hood application in automotive industry. *Journal of Vinyl and Additive Technology*, 2022, Properties, chemistry, and mode of action of antioxidants in thermoplastics and rubbers: Recent developments, 28 (2), pp.418-429. <10.1002/vnl.21916>. <hal-03709249>

HAL Id: hal-03709249

<https://hal.science/hal-03709249v1>

Submitted on 29 Jun 2022

HAL is a multi-disciplinary open access archive for the deposit and dissemination of scientific research documents, whether they are published or not. The documents may come from teaching and research institutions in France or abroad, or from public or private research centers.

L'archive ouverte pluridisciplinaire **HAL**, est destinée au dépôt et à la diffusion de documents scientifiques de niveau recherche, publiés ou non, émanant des établissements d'enseignement et de recherche français ou étrangers, des laboratoires publics ou privés.



HAL Authorization

Thermal aging of electrical cable insulation made of cross-linked low density polyethylene for under-hood application in automotive industry

Tetiana Salivon^{1,2} | Raphael Comte² | Xavier Colin¹ 

¹PIMM, Arts et Métiers Institute of Technology, CNRS, CNAM, HESAM University, Paris, France

²PSA PEUGEOT CITROEN, Technical Center of Vélizy, EES Department, Vélizy-Villacoublay, France

Correspondence

Xavier Colin, PIMM, Arts et Métiers Institute of Technology, CNRS, CNAM, HESAM University, 151 boulevard de l'Hôpital, 75013 Paris, France.
Email: xavier.colin@ensam.eu

Abstract

The thermal aging of two electrical cable insulations made of cross-linked low density polyethylene (XLPE) only differing by their stabilization system was studied in air between 125 and 200°C. The chemical consumption of the two types of antioxidants (phenol and sulfide), the build-up of oxidation products and the consequences of thermal oxidation on the mechanical properties were respectively determined by measurement of the oxidation induction time (OIT), Fourier transform infrared spectroscopy (FTIR) and uniaxial tensile testing. It was found that the chemical consumption of each antioxidant occurs in turn almost independently, starting with the sulfide antioxidant and involving small but well detectable antagonistic effects. As soon as the antioxidant concentration becomes very low, that is, practically undetectable by OIT measurements, the thermal oxidation of XLPE is detected by FTIR spectroscopy causing a catastrophic decrease in the fracture properties. It was shown that the complete consumption of antioxidants coincides with the end of the oxidation induction period and the onset of the sudden decrease in the elongation at break. Based on all these experimental results, a simplified kinetic model was developed to account as faithfully as possible for the consumption kinetics of antioxidants, evaluate their antagonistic effects and, using a relevant end-of-life criterion, predict the lifetime of the two XLPE insulations. It was found a satisfying agreement between theory and experiment.

KEYWORDS

antagonist effects, cross-linked polyethylene, embrittlement, kinetic modeling, lifetime prediction, stabilization, thermal oxidation

1 | INTRODUCTION

Today, bundles of electrical cables represent between 40% and 50% of the weight of an automotive vehicle propelled by a combustion engine. Put end to end, the total length of cables can reach 2 km.^[1] In order to lower the weight and production costs of vehicles, but also their carbon footprint, the design offices of automobile

manufacturers are considering the possibility of reducing the safety factors used for the sizing of electrical cables. Before embarking on this strategy, it is crucial to check that it will not adversely affect the in-service operation and the lifetime of the entire electrical system.

A reduction in the circular section of the electric cable necessarily leads to a reduction in the thickness of its outer insulating layer, generally made of cross-linked

low density polyethylene (XLPE) or plasticized poly(vinyl chloride). However, this outer layer is the most vulnerable part in an electric cable. Indeed, hydrocarbon polymers are known to be very sensitive to the thermochemical attacks from the external environment, in particular to thermal oxidation.^[2-4] In order to preserve their functional properties at long term, hydrocarbon polymers are generally protected against thermal oxidation by one or more antioxidants.^[5-13] In a first approach, only two main types of antioxidants can be distinguished.^[5-9,13] They differ essentially in their general chemical structure and thus, in their main stabilization mechanism. These two types of antioxidants are free radical scavengers and hydroperoxide decomposers. The first ones are also called “primary antioxidants” or “chain breaking antioxidants” as they increase the termination rate by reacting with the peroxy radicals formed during the propagation stage of the oxidation reaction and thus, efficiently interrupt the radical chain propagation. They are generally hindered phenols and secondary aromatic amines. In contrast, the second ones are called “secondary antioxidants” or “preventive antioxidants” as they reduce the initiation rate by converting the hydroperoxides into non-radical products and thus, efficiently delay the auto-accelerated character of thermal oxidation. They are typically organic phosphites and sulfides.

Many kinetic models have been developed to predict the thermal aging of the insulating layer of electric cables since the early 1980s. Some of these models have been improved several times^[14-19] and are now able to predict with a great accuracy the oxidation of polymers and the consequences of this oxidation on their use properties, for example on their mechanical^[20] and dielectric properties.^[21] As sophisticated as they are, these models still do not take into account the effects of antioxidants so that, at this stage, they are unable to predict the long induction period preceding the onset and sharp acceleration of oxidation. However, in the mid-1980s, Emmanuel and Buchachenko had proposed a simplified, but very interesting approach, for modeling the chemical consumption kinetics of antioxidants.^[22]

The purpose of this article is twofold. First of all, the thermal aging in air of two XLPE formulations, commonly used as outer insulating layer of electrical cables in the automotive industry, will be assessed in the temperature range recommended by the ISO 6722 standard according to their thermal class,^[23] typically:

- Between 125 and 175°C for XLPE of thermal class C (denoted XLPE-C),
- Between 150 and 200°C for XLPE of thermal class D (denoted XLPE-D).

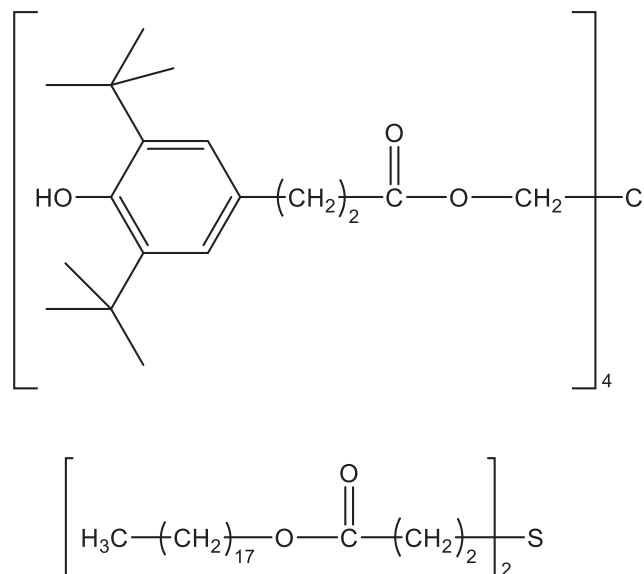


FIGURE 1 Chemical formulas of Irganox 1010 (top) and Irganox PS 802 FL (bottom)

It should be pointed out that these two XLPE formulations only differ in their stabilization system that is specially adapted to their thermal class. Indeed, XLPE-C is only stabilized by a hindered phenol (with commercial name Irganox 1010) while XLPE-D is stabilized by a blend of two antioxidants, composed of the same primary antioxidant in the same quantity (Irganox 1010) but now associated with an organic sulfide (Irganox PS 802 FL). As an information, the chemical structures of these two antioxidants are reported in Figure 1. Consequently, comparing the stabilization efficiency in the two XLPE formulations at the same exposure temperatures (for instance, at 150 and 175°C) will allow investigating the possible synergistic or antagonistic effects between these two types of antioxidants. In addition, increasing to 200°C the upper temperature boundary recommended by the ISO 6722 standard for XLPE-C will allow selecting additional exposure temperatures for this comparison.

In addition to the consumption of antioxidants, the oxidation of the two XLPE insulations and the consequences of oxidation on their mechanical properties, in particular on their fracture properties, will be investigated.

Then, based on these experimental results, a kinetic model will be developed to account as faithfully as possible for the consumption kinetics of antioxidants and, using a relevant end-of-life criterion, predict the lifetime of the two XLPE insulations. The kinetic model will be derived from the approach of Emanuel and Buchachenko.^[22]

2 | EXPERIMENTAL

2.1 | Materials

Two single-core electrical cables with a XLPE insulating layer of $560 \pm 30 \mu\text{m}$ thick were supplied by ACOME company. Photographs of these cables are provided in Figure 2. The formulations of the two XLPE insulations, as well as their main physicochemical properties prior to thermal aging, are reported in Table 1.

Apart from the pigmentation of their outer surface, these two XLPE formulations differ in their stabilization system that is specially adapted to their thermal class. Indeed, the oxidation induction time (OIT) measured under pure oxygen at 220 and 240°C is about four times higher for XLPE-D compared to XLPE-C. This result highlights the real interest of using blends of primary plus secondary antioxidants in industrial formulations in view of increasing their thermal stability and lifetime. Concerning blends of phenol plus thioester antioxidants in PE, note that synergistic effects were regularly reported in the literature over the past half-century.^[24–30]

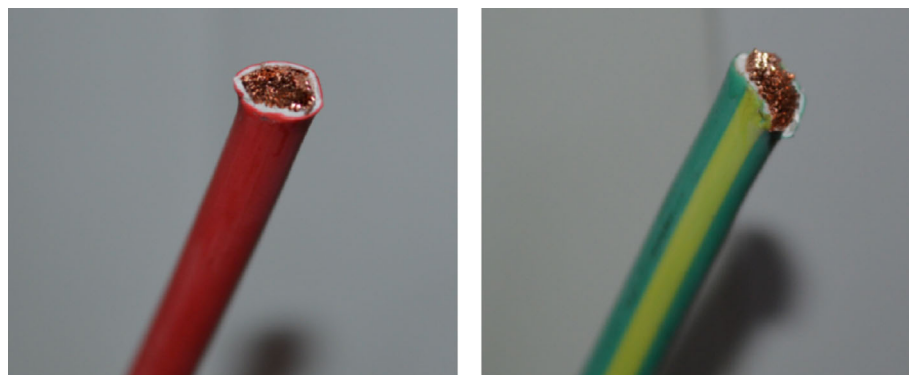


FIGURE 2 Single-core electrical cables with XLPE-C (left) and XLPE-D insulation (right)

2.2 | Thermal aging conditions

The two XLPE insulations were separated from the conductive core using a wire stripper before being thermally aged in air-ventilated ovens at four different temperatures, previously defined according to the ISO 6722 standard.^[23] These four temperatures are reported in Table 2.

2.3 | Characterization after thermal aging

For each aging temperature, the XLPE insulations were frequently removed from the air-ventilated ovens and

TABLE 2 Thermal aging temperatures of XLPE insulations

Insulation reference	Temperature (°C)			
XLPE-C	125	150	175	200
XLPE-D	150	160	175	200

Note: The temperatures used to compare their long-term behavior are written in bold.

Abbreviation: XLPE, cross-linked low density polyethylene.

TABLE 1 Formulations and main physico-chemical properties of XLPE insulations

Insulation reference		XLPE-C	XLPE-D
Formulations	Pigments	Pink	Green and yellow
	Mineral fillers	Talc (35 wt%)	Talc (40 wt%)
	Primary antioxidant	Irganox 1010	Irganox 1010
	Secondary antioxidant	None	Irganox PS 802 FL
Physico-chemical properties	Thermal class ^[23]	C	D
	Melting point (T_m)	123°C	122°C
	Crystallinity ratio (X_C)	23%	13%
	OIT (at 220°C)	272 min	540 min
	OIT (at 240°C)	68 min	152 min

Abbreviations: OIT, oxidation induction time; XLPE, cross-linked low density polyethylene.

cooled at room temperature in the dry atmosphere of a desiccator (containing silica gel) before being analyzed by complementary physico-chemical laboratory techniques.

The residual global concentration of active antioxidants ([AO]) in the XLPE insulations was estimated from the measurement of the OIT assuming the existence of a proportionality between both quantities^[31–33]:

$$\text{OIT} = K_{\text{OIT}}[\text{AO}] + \text{OIT}_{\text{Uns}} \quad (1)$$

where, K_{OIT} is a constant depending on the temperature and the couple (polymer matrix, antioxidants) under consideration, and OIT_{Uns} is the value of the unstabilised XLPE insulation under consideration. For temperature typically higher than 200°C, OIT_{Uns} is generally near zero. Equation 1 can thus be rewritten:

$$\text{OIT} = K_{\text{OIT}}[\text{AO}] \quad (2)$$

OIT measurements were performed under a pure oxygen flow (50 ml min⁻¹) at 240°C using a TA Instrument DSC Q20 calorimeter. This temperature was chosen in order to have an acceptable duration of experiments (typically less than 3 h) for both unaged and slightly aged XLPE insulations. Samples of about 5 mg were introduced in open standard aluminum pans. The samples were first heated under a pure nitrogen flow (50 ml min⁻¹) from room temperature to 240°C with a heating rate of 10°C min⁻¹. After an isotherm segment of 5 min for temperature equilibration, the gas flow was switched from nitrogen to oxygen. An isotherm at 240°C was then performed under a pure oxygen flow in order to access the OIT at this temperature. The OIT value was determined using the tangent method, which corresponds to the duration period between the introduction of the oxygen flow in the DSC cavity and the onset of the oxidation exotherm.

The concentration of oxidation products (mainly carbonyls) after the induction period was estimated by Fourier transform infra-red spectroscopy (FTIR) in an attenuated reflectance mode (ATR). FTIR spectra were recorded at room temperature between 4000 and 650 cm⁻¹ using a Perkin Elmer FTIR Frontier device equipped with a diamond/ZnSe crystal, after averaging the 16 scans obtained with a resolution of 4 cm⁻¹.

It should be recalled that there is a wide variety of carbonyl products formed during the thermal aging of hydrocarbon polymers. In PE, independently of its macromolecular structure (i.e., linear, branched or chemically crosslinked), the resulting carbonyl composite band is generally centered at 1714–1715 cm⁻¹ in the IR spectra^[20,34–39] due to the much high value of the coefficient of molar extinction of carboxylic acids compared to other

carbonyl products.^[37] However, due to the presence of several types of metal oxides in the outer surface of the XLPE insulations under study, as soon as they were formed, many carboxylic acids were converted into carboxylates during the thermal exposure, according to the well-known reactions reported for instance in Reference [40].

Examples of FTIR spectra obtained for XLPE-C before and after a few thousand hours of thermal exposure in air at 150°C are shown in Figure 3. These spectra highlight three major behavioral trends:

- The initial presence of an intense band at about 1731 cm⁻¹ assigned to stretching vibration of the C=O bond of carbonyl groups (such as esters) in organic pigments,^[41] which seems to slowly decrease during the thermal exposure, thus demonstrating that these pigments are not completely stable at such high temperatures.
- The appearance and growth of two shoulders at about 1714 and 1773 cm⁻¹, respectively assigned to the stretching vibration of the C=O bond in carboxylic acids (not yet converted into carboxylates) and γ -lactones or anhydrides, which have been formed on the XLPE structure.
- The appearance and growth of two well-known bands for the stretching vibration of the C=O bond in metal carboxylates at about 1654 and 1595 cm⁻¹,^[42] resulting from the consumption of carboxylic acids by several metal oxides.

The absorbance of carboxylates at about 1595 cm⁻¹ was chosen to determine the oxidation kinetics of XLPE in the present study. It should be recalled that, in principle, FTIR in ATR mode is not a quantitative technique because large absorbance variations can be measured for a same sample depending on many factors: penetration depth of the IR beam, surface aspect of the sample (roughness, color, etc.), spatial distribution of pigments and fillers, and so forth. To try to eliminate all these variations, it was decided to normalize the absorbance of carboxylates by the absorbance of a band completely insensitive to thermal aging, which can thus be chosen as reference band: the stretching vibration of the Si—O—Si group in talc at about 1020 cm⁻¹.^[43] Consequently, the concentration of carboxylates can simply be estimated from the following equation derived from the common Beer–Lambert's law:

$$[\text{Carboxylates}] = K \frac{\text{Abs}_{1595 \text{ cm}^{-1}}}{\epsilon_{1595 \text{ cm}^{-1}} \times \text{Abs}_{1020 \text{ cm}^{-1}}} \quad (3)$$

where, $\text{Abs}_{1595 \text{ cm}^{-1}}$ and $\text{Abs}_{1020 \text{ cm}^{-1}}$ are respectively the absorbances of the bands at about 1595 and 1020 cm⁻¹,

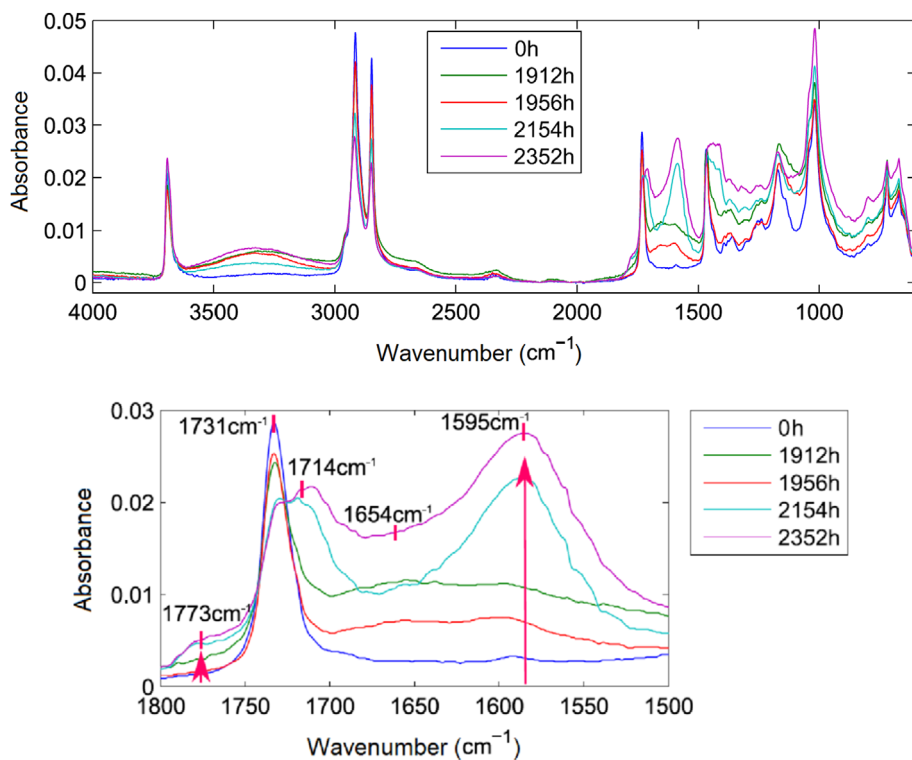


FIGURE 3 Changes in the FTIR spectrum of XLPE-C during its thermal exposure in air at 150°C. Top: Full IR spectra. Bottom: Zoom of the carbonyl region. FTIR, Fourier transform infrared spectroscopy

$\epsilon_{1595\text{ cm}^{-1}}$ is the coefficient of molar extinction at 1595 cm^{-1} , and K is a constant depending on the coefficient of molar extinction at 1020 cm^{-1} , the amount of talc in XLPE and the ratio between the penetration depths of the IR beam in XLPE at the two wavenumbers under consideration.

The value of $\epsilon_{1595\text{ cm}^{-1}}$ previously reported in literature for ammonium carboxylates was retained for this study: $\epsilon_{1595\text{ cm}^{-1}} \approx 330\text{ L mol}^{-1}\text{ cm}^{-1}$.^[37] In contrast, the value of K was estimated so as to find, with the general Equation 3, the initial concentration of C—H bonds in XLPE, that is, $[\text{C—H}] \approx 60\text{ mol L}^{-1}$, using the closest IR bands to 1595 cm^{-1} whose coefficient of molar extinction is well-known in literature.^[44] Our attention naturally focused on the band of the CH_2 scissoring vibration at about 1466 cm^{-1} for which $\epsilon_{1466\text{ cm}^{-1}} \approx 4\text{ L mol}^{-1}\text{ cm}^{-1}$.^[44] The following estimates were obtained for K : $\approx 510\text{ cm}^{-1}$ for XLPE-C and $\approx 250\text{ cm}^{-1}$ for XLPE-D.

The consequences of thermal oxidation on mechanical properties were investigated by uniaxial tensile testing on small dumb-bell samples taken with a punch in the XLPE insulations before their thermal exposure. These samples were 34 mm long, 4 mm large at both extremities and 0.56 mm thick. The useful rectangular part between the two sample heads (i.e., where failure occurs in tension) was 10 mm long, 2 mm wide and 0.56 mm thick. These samples were progressively loaded in tension using an Instron 6799 machine equipped with a 10 kN load cell and pneumatic jaws, with a constant crosshead

speed of 20 mm min^{-1} until their breaking point, at which their ultimate elongation was calculated.

3 | RESULTS AND INTERPRETATION

3.1 | Antioxidant consumption

As expected, a long oxidation induction period is first observed for both XLPE formulations regardless of their exposure temperature, during which the antioxidants are progressively chemically consumed by trying to block and delay the thermal oxidation. As an example, the consumption kinetics of antioxidants in the two XLPE formulations are compared in Figure 4 for thermal exposures in air at 150, 175, and 200°C. To be able to explain both behavioral similarities and differences, it should be recalled that XLPE-C only contains a phenol antioxidant (Irganox 1010), whereas XLPE-D contains a blend of this phenol antioxidant with a sulfide antioxidant (Irganox PS 802 FL).

It clearly appears that the consumption of the phenol antioxidant in XLPE-C occurs in one single kinetic stage, the rate of which progressively slowing down over time of exposure to finally cancel out at the same time as the phenol concentration. Such a consumption kinetics seems to be consistent with the main action mechanism of phenol antioxidants reported in literature, for example, in Reference [13]:

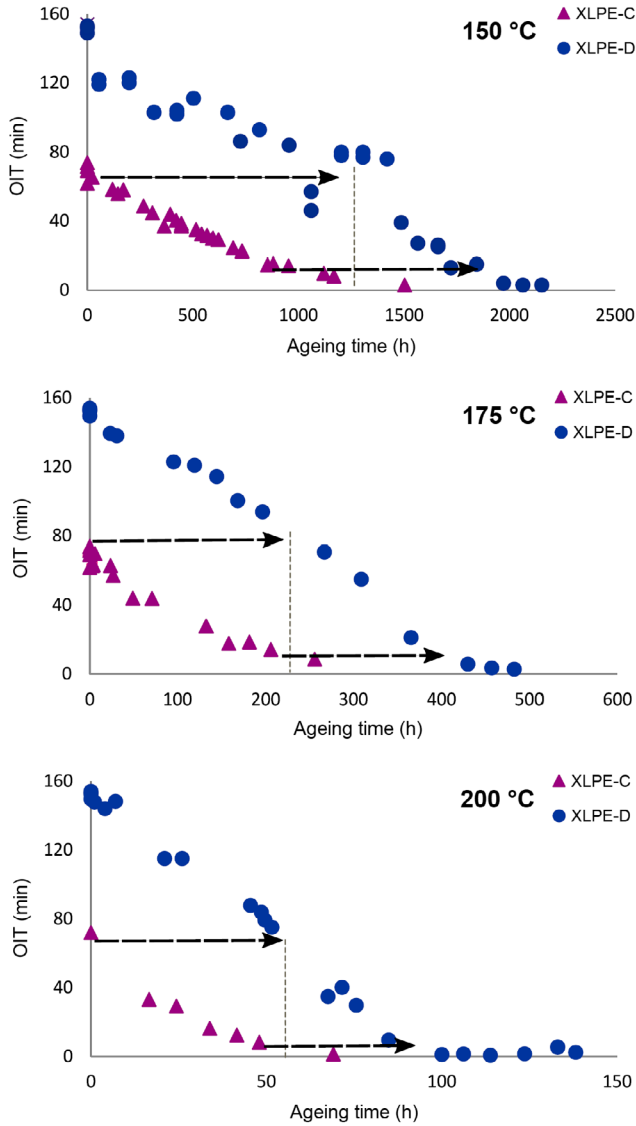
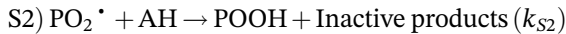


FIGURE 4 Comparison of the consumption kinetics of antioxidants in the two XLPE insulations in air at 150, 175, and 200°C. XLPE, cross-linked low density polyethylene



where, AH designates a phenol group and k_{S2} is the corresponding rate constant.

The consumption rate can thus be written as follows:

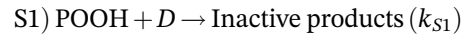
$$\frac{d[AH]}{dt} = -n_{AH}k_{S2}[PO_2 \cdot][AH] \quad (4)$$

where, n_{AH} is the number of phenol groups carried by the antioxidant molecule (i.e., its functionality). For Irganox 1010, $n_{AH} = 4$ (see Figure 1).

In XLPE-D, in contrast, the consumption of the blend of phenol and sulfide antioxidants occurs in two distinct and successive kinetic stages. It is clear that the second

stage displays exactly the same shape as the consumption curves of phenol antioxidant just described for XLPE-C. It is thus logically assigned to the consumption of the phenol antioxidant alone. However, it is now shifted to longer times due to the protective effect of the sulfide antioxidant. By deduction, the first kinetic stage is then assigned to the complete consumption of the sulfide antioxidant. At this stage of the investigations, it is very difficult to know if significant synergistic or antagonistic effects between these two antioxidants occur during the first stage. Indeed, it would rather seem that they act separately, each in turn, starting with the sulfide antioxidant.

As already seen for the second kinetic stage, the rate of the first stage progressively slows down over time of exposure to finally cancel out presumably at the same time as the sulfur concentration. Here also, this consumption kinetics seems to be consistent with the main action mechanism of sulfide antioxidants reported in literature, for example, in Reference [13]:



where, D designates the sulfur group and k_{S1} is the corresponding rate constant.

The consumption rate can thus be written:

$$\frac{d[D]}{dt} = -k_{S1}[POOH][D] \quad (5)$$

The time required for the complete consumption of antioxidants (denoted t_{AO}) in air between 125 and 200°C in both XLPE formulations is reported in Table 3. It obeys an Arrhenius law with a similar activation energy ($E_a \approx 102 \text{ kJ mol}^{-1}$) for both XLPE formulations. It can thus be concluded that the stabilization efficiency only differs through the value of the pre-exponential factor, which is about 1.4 times higher for XLPE-D compared to XLPE-C. The values of the Arrhenius parameters determined between 125 and 200°C for both XLPE formulations are reported in Table 4.

3.2 | Thermal oxidation and embrittlement

As soon as the antioxidant concentration becomes very low, that is, practically undetectable by OIT measurements, several carbonyl bands start to be detected by FTIR spectroscopy in both XLPE formulations. In particular, as already shown in Figure 3, the rapid growth of a carboxylate band is clearly observed at about 1595 cm^{-1} in the FTIR spectra. The concentration of carboxylates in air between 125 and

T ($^{\circ}\text{C}$)	XLPE-C				XLPE-D			
	t_{AO} (h)	t_i (h)	t_{FI} (h)	t_{F50} (h)	t_{AO} (h)	t_i (h)	t_{FI} (h)	t_{F50} (h)
125	8100	8000	8000	–	–	–	–	–
150	1500	1600	1600	2050	1900	2500	2500	3250
160	–	–	–	–	1080	1080	1230	1860
175	300	350	350	380	420	430	470	530
200	60	60	50	65	90	100	80	110

Abbreviation: XLPE, cross-linked low density polyethylene.

TABLE 4 Pre-exponential factor (P_0) and activation energy (E_a) for the different characteristic times of the thermal oxidation and embrittlement kinetics of the two XLPE insulations in air between 125 and 200 $^{\circ}\text{C}$

	XLPE-C			XLPE-D		
	t_{AO}	t_i	t_{FI}	t_{AO}	t_i	t_{FI}
P_0 (h)	3.5×10^{-10}	4.8×10^{-10}	1.8×10^{-10}	4.8×10^{-10}	2.1×10^{-10}	2.5×10^{-10}
E_a (kJ mol $^{-1}$)	102	101	104	102	106	105

Abbreviation: XLPE, cross-linked low density polyethylene.

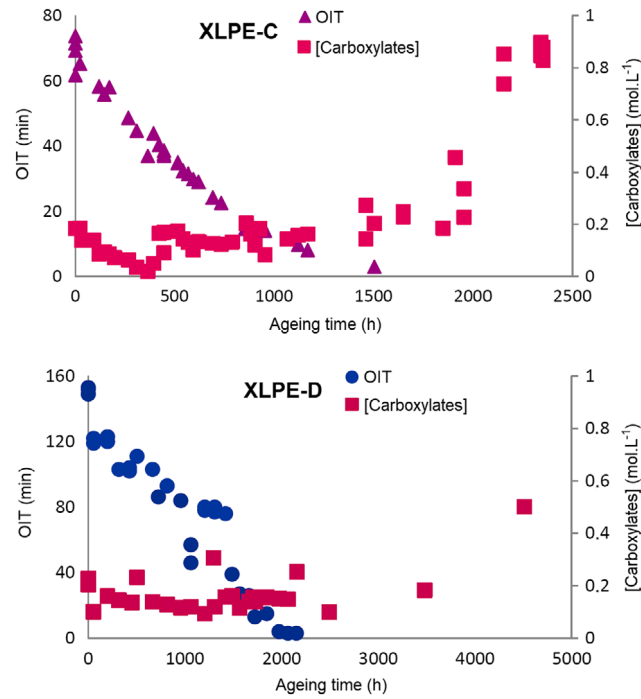


FIGURE 5 Comparison of the build-up kinetics of carboxylates and the consumption kinetics of antioxidants in the two XLPE insulations in air at 150 $^{\circ}\text{C}$. XLPE, cross-linked low density polyethylene

200 $^{\circ}\text{C}$ was determined with Equation (3), then plotted against time of exposure. As an example, the build-up kinetics of carboxylates and the consumption kinetics of antioxidants in both XLPE formulations are compared in Figure 5 for thermal exposure in air at 150 $^{\circ}\text{C}$.

TABLE 3 Time for the complete consumption of antioxidants (t_{AO}), duration of the oxidation induction period (t_i), and times at the onset (t_{FI}) and within the embrittlement transition (t_{F50}) for the two XLPE insulations aged in air between 125 and 200 $^{\circ}\text{C}$

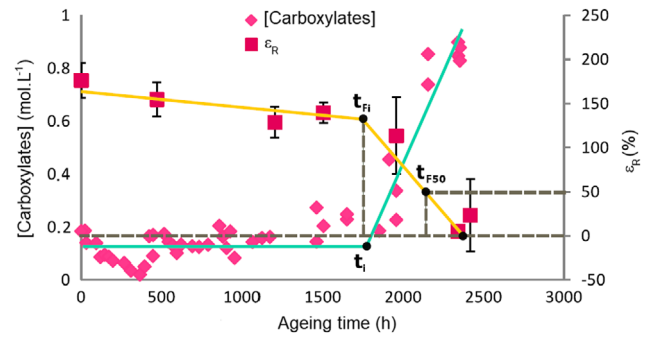


FIGURE 6 Comparison of the thermal oxidation and embrittlement kinetics in XLPE-C in air at 150 $^{\circ}\text{C}$

The duration of the oxidation induction period (denoted t_i) is reported in Table 3 for both XLPE formulations. As t_i is roughly equal to t_{AO} , it also obeys an Arrhenius law with almost the same values of activation energy and exponential factor as t_{AO} (see Table 4).

As soon as oxidation starts to be detected, the fracture properties of both XLPE formulations start to decrease catastrophically. An interesting observation is that the onset of the sudden decrease in the elongation at break seems to coincide with the end of the oxidation induction period (see Figure 6). That is the reason why, in this study, two end-of-life criteria were chosen to estimate the lifetime of XLPE insulations: one corresponding to the onset of embrittlement and another corresponding to the conventional end-of-life criterion in cable industry, that is, the reduction of 50% in the initial value of the elongation at break.^[16,19] The respective estimates of lifetime were denoted t_{FI} and t_{F50} .

The values of t_{Fi} and t_{F50} are also reported in Table 3 for both XLPE formulations. The following correlations were found between the characteristic times of the thermal oxidation and embrittlement kinetics:

$$t_{Fi} \approx t_i \approx t_{AO} \quad (6)$$

and

$$t_{F50} \approx 1.3 \times t_{Fi} \quad (7)$$

As t_{Fi} and t_{F50} are respectively equal and proportional to t_{AO} , they also obey an Arrhenius law with almost the same values of activation energy and exponential factor as t_{AO} (see Table 4).

This kinetic analysis leads to the main conclusion that it is enough to model the consumption kinetics of antioxidants to predict the lifetime of the two XLPE insulations. This work constitutes the objective of the next paragraph.

4 | KINETIC MODELING

4.1 | XLPE-C

For each type of antioxidants, a relatively simple kinetic model can be derived from their main action mechanism (i.e., from the reactions S1 and S2 recalled in previous section) if making simplifying assumptions.

In particular, if assuming a steady state regime for peroxy radicals, a simple integration of Equation (4) between 0 and t leads to:

$$[AH] = [AH]_0 \text{Exp}(-K_{S2}t) \quad (8)$$

where, $K_{S2} = n_{AH}k_{S2}[PO_2^*]$ is an apparent first-order rate constant, and $[AH]_0$ is the initial concentration of phenol groups in both XLPE insulations.

Introducing now Equation (8) into Equation (2) leads to:

$$\text{OIT} = \text{OIT}_0 \text{Exp}(-K_{S2}t) \quad (9)$$

where, OIT_0 is the initial value of OIT reported in Table 1 for XLPE-C. At 240°C, $\text{OIT}_0 = 68$ min.

The simulations with Equation (9) of the changes in OIT in air between 125 and 200°C for XLPE-C are shown in Figure 7. It can be seen that the consumption of the phenol antioxidant really obeys a first-order kinetics, as predicted by Equation (8).

The values of the rate constant K_{S2} used for these simulations are reported in Table 5. As expected, K_{S2} obeys

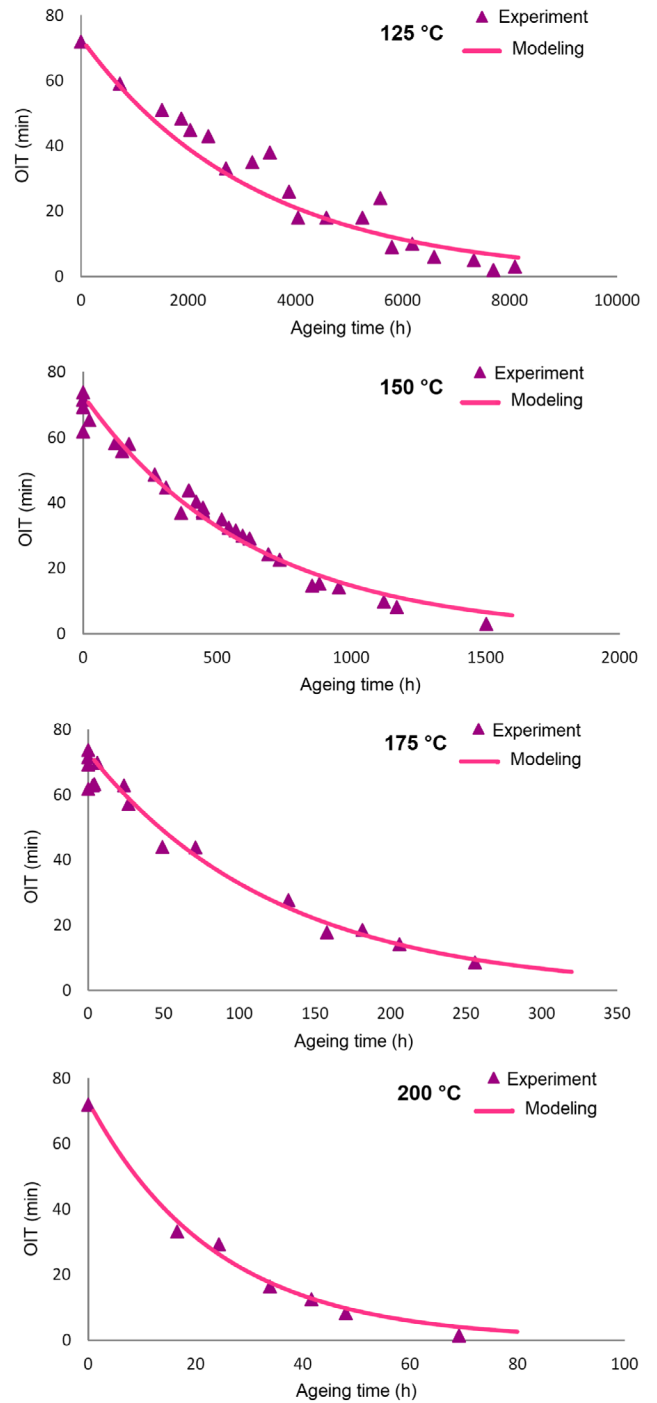


FIGURE 7 Simulation with Equation (9) of the changes in OIT in air at 125, 150, 175, and 200°C for XLPE-C. OIT, oxidation induction time

an Arrhenius with the same activation energy as t_{AO} , that is, 102 kJ mol^{-1} (see Table 6).

If considering now that the antioxidant is completely consumed when OIT reaches the order of magnitude of the detection threshold of the OIT measurement technique, that is, typically 1 min, it can be written:

T (°C)	XLPE-C	XLPE-D			
	K_{S2} (s ⁻¹)	K_{S1} (s ⁻¹)	K_{S2} (s ⁻¹)	t_D (h)	$\pm\Delta OIT$ (min)
125	8.6×10^{-8}	-	-	-	-
150	4.4×10^{-7}	3.5×10^{-7}	1.3×10^{-6}	1350	-17
160	-	6.0×10^{-7}	2.7×10^{-6}	796	-17
175	2.2×10^{-6}	1.2×10^{-6}	4.4×10^{-6}	288	-18
200	1.2×10^{-5}	7.8×10^{-6}	2.9×10^{-5}	63	-18

Abbreviation: XLPE, cross-linked low density polyethylene.

	XLPE-C	XLPE-D		
	K_{S2} (s ⁻¹)	K_{S1} (s ⁻¹)	K_{S2} (s ⁻¹)	t_D (h)
P_0	2.0×10^6	1.5×10^6	3.1×10^6	2.5×10^{-10}
E_a (kJ mol ⁻¹)	102	103	100	103

Abbreviation: XLPE, cross-linked low density polyethylene.

$$1 \text{ min} = OIT_0 \text{Exp}(-K_{S2}t_{AO}) \quad (10)$$

$$\text{i.e. } t_{AO} = \frac{-1}{K_{S2}} \text{Ln}\left(\frac{1}{OIT_0}\right) \quad (11)$$

$$\text{i.e. } t_{AO} = \frac{1}{K_{S2}} \text{Ln}(OIT_0) \quad (12)$$

Finally, the lifetime of XLPE-C insulation can simply be estimated as follows:

$$t_{F50} \approx \frac{1.3}{K_{S2}} \text{Ln}(OIT_0) \quad (13)$$

4.2 | XLPE-D

By analogy, if assuming a steady state regime for hydroperoxides, a simple integration of Equation (5) between 0 and t leads to:

$$[D] = [D]_0 \text{Exp}(-K_{S1}t) \quad (14)$$

where, $K_{S1} = k_{S1}[\text{POOH}]$ is an apparent first-order rate constant and $[D]_0$ is the initial concentration in sulfur groups in XLPE-D.

Introducing now Equation (14) into Equation (2) leads to:

$$OIT = OIT_0 \text{Exp}(-K_{S1}t) \quad (15)$$

TABLE 5 Values of the parameters used for modeling the antioxidant consumption and predicting the lifetime of both XLPE insulations in air between 125 and 200°C

TABLE 6 Pre-exponential factor (P_0) and activation energy (E_a) for the different parameters used for modeling the antioxidant consumption and predicting the lifetime of both XLPE insulations in air between 125 and 200°C

In previous section (see Figure 4), it was shown that, in XLPE-D, the consumption of the blend of phenol and sulfide antioxidants occurs in two distinct and successive kinetic stages, each one being assigned, in a first approach, to the complete consumption of each antioxidant alone, starting with the sulfide antioxidant. For XLPE-D, OIT is thus the sum of two contributions:

$$OIT = OIT_1 \times \theta(t_D - t) + OIT_2 \times \theta(t - t_D) \quad (16)$$

where, OIT_1 and OIT_2 are respectively the changes in OIT during the first and second kinetic stages, t_D is the boundary between these two stages, and $\theta(t)$ is the Heaviside function allowing to define the changes in OIT during each stage.

Equation (16) can then be rewritten such as:

$$OIT = (OIT_D + OIT_{AH,0} \pm \Delta OIT) \times \theta(t_D - t) + OIT_{AH} \times \theta(t - t_D) \quad (17)$$

where, OIT_D and OIT_{AH} are the changes in OIT due to the consumption of sulfur and phenol groups, respectively described by Equations 9 and 15, $OIT_{AH,0}$ is the initial value of OIT_{AH} reported in Table 1 (at 240°C, $OIT_{AH,0} = 68$ min) and $\pm\Delta OIT$ designates possible synergistic or antagonistic effects during the first kinetic stage.

Introducing Equations (9) and (15) into Equation (17) leads to:

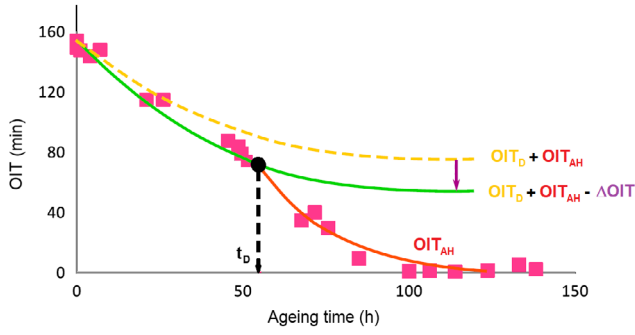


FIGURE 8 Highlighting of antagonistic effects between the two types of antioxidants when attempting to model their consumption kinetics. Example of simulation in air at 200°C for XLPE-D

$$\text{OIT} = (\text{OIT}_{D,0}\text{Exp}(-K_{S1}t) + \text{OIT}_{\text{AH},0} \pm \Delta\text{OIT}) \times \theta(t_D - t) + \text{OIT}_{\text{AH},0}\text{Exp}(-K_{S2}(t - t_D)) \times \theta(t - t_D) \quad (18)$$

where, $\text{OIT}_{D,0}$ is the initial value of OIT_D , which is simply deduced from the initial value of OIT reported in Table 1 for XLPE-D (at 240°C, $\text{OIT}_0 = 152$ min) such as:

$$\text{OIT}_{D,0} = \text{OIT}_0 - \text{OIT}_{\text{AH},0} \pm \Delta\text{OIT} \quad (19)$$

From the very first simulations, it appeared that it was necessary to add antagonistic effects between the two types of antioxidants during the first kinetic stage, that is, a negative term $-\Delta\text{OIT}$, as illustrated in Figure 8.

The final simulations with Equation (17) of the changes in OIT in air between 150 and 200°C for XLPE-D are shown in Figure 9. It can be seen that the consumptions of both the sulfide and phenol antioxidants really obey first-order kinetics, as predicted by Equation (17).

The values of the rate constant K_{S1} and K_{S2} , the interaction parameter $\pm\Delta\text{OIT}$ between both types of antioxidants, and the boundary time t_D between both kinetic stages used for these simulations are also reported in Table 5. They call for the following comments:

- Values of K_{S2} about 2–3 times higher were determined for XLPE-D compared to XLPE-C, which can be interpreted as a new evidence of antagonistic effects between the two types of antioxidants.
- As expected, K_{S1} also obeys an Arrhenius with a similar activation energy as K_{S2} , typically 103 kJ mol^{-1} (see Table 6).
- As expected, for all the exposure temperatures under investigation, the transition between the first and second kinetic stage takes place when OIT reaches a value of 70 ± 2 min, which roughly corresponds to the value

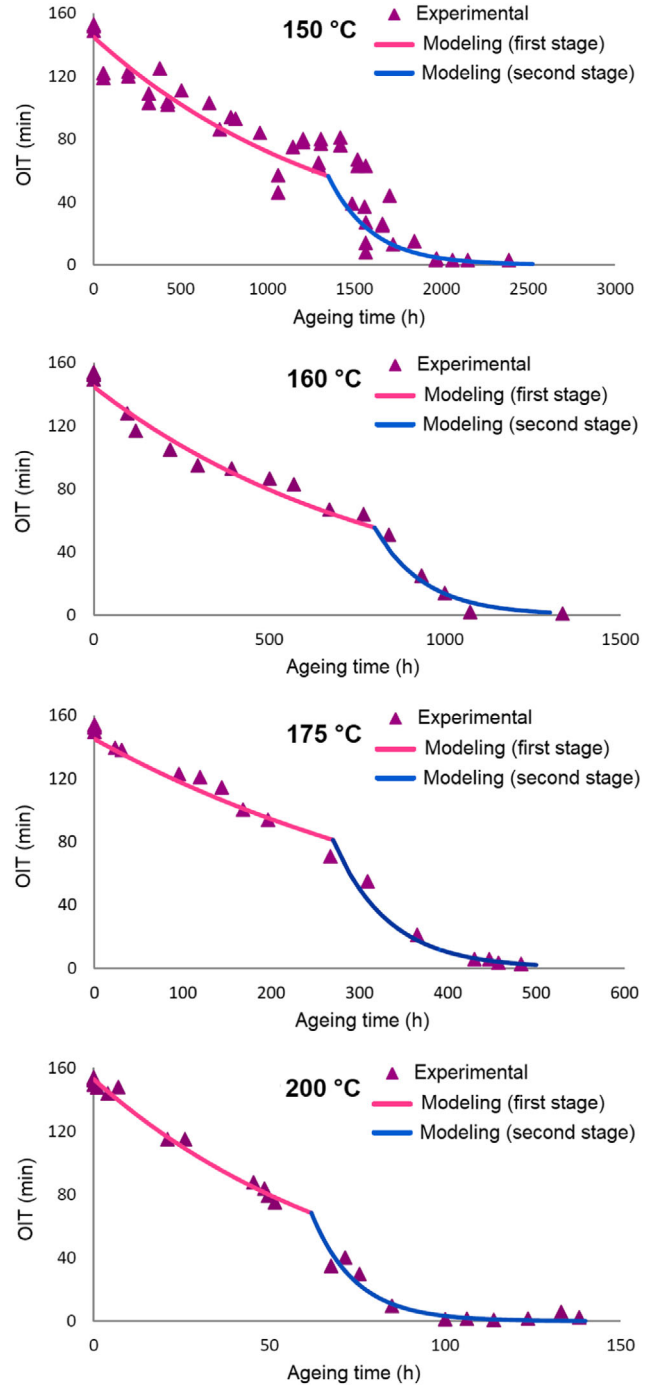


FIGURE 9 Simulation with Equation (17) of the changes in OIT in air at 150, 160, 175, and 200°C for XLPE-D. OIT, oxidation induction time

of $\text{OIT}_{\text{AH},0}$ reported in Table 1 ($\text{OIT}_{\text{AH},0} = 68$ min). The corresponding time t_D obeys an Arrhenius law with the same activation energy as K_{S1} (see Table 6).

- For all the exposure temperatures under investigation, the antagonistic effects between the two types of antioxidants $-\Delta\text{OIT}$ is estimated at about -18 min. They correspond to a reduction of about 11% in the

stabilization efficiency in XLPE-D. The application of Equation 19 leads to a value of $OIT_{D,0}$ of about 102 min. However, it is surprising to find that these antagonistic effects are completely independent of temperature. Further experiments are needed to understand and explain this peculiar behavior.

Applying the same reasoning as for the calculation of t_{AO} of XLPE-C, it is now possible to determine t_D :

$$1 \text{ min} = OIT_{D,0} \text{Exp}(-K_{S1}t_D) - \Delta OIT \quad (20)$$

$$\text{i.e. } t_D = \frac{1}{K_{S1}} \text{Ln} \left(\frac{OIT_{D,0}}{1 + \Delta OIT} \right) \quad (21)$$

In the case of XLPE-D, t_{AO} is reached at the end of the two kinetic stages, that is, after a duration corresponding to the sum of the two characteristic times previously determined with Equations 12 and 21:

$$t_{AO} = \frac{1}{K_{S1}} \text{Ln} \left(\frac{OIT_{D,0}}{1 + \Delta OIT} \right) + \frac{1}{K_{S2}} \text{Ln}(OIT_{AH,0}) \quad (22)$$

Finally, the lifetime of the XLPE-D insulation can be estimated as follows:

$$t_{F50} \approx \frac{1.3}{K_{S1}} \text{Ln} \left(\frac{OIT_{D,0}}{1 + \Delta OIT} \right) + \frac{1.3}{K_{S2}} \text{Ln}(OIT_{AH,0}) \quad (23)$$

5 | CONCLUSION

The stabilization efficiency in the two XLPE insulations was investigated in air between 125 and 200°C by OIT measurements. It was found that the chemical consumption of each antioxidant occurs almost independently.

In XLPE-D, the consumption of the blend of phenol and sulfide antioxidants starts with the sulfide antioxidant, which decomposes the hydroperoxides in a non-radical way and thus, protects the phenol antioxidant from the radical attack. Small but well detectable antagonistic effects, corresponding to a reduction of about 11% in the stabilization efficiency in XLPE-D, were highlighted between the two types of antioxidants during this first kinetic stage. The consumption of the phenol antioxidant was observed to start when the sulfide antioxidant had almost completely disappeared.

It was also found that the thermal oxidation of XLPE starts when the antioxidant concentration becomes very low, that is, practically undetectable by OIT measurements. Thenceforth, the fracture

properties decrease catastrophically and the lifetime of XLPE insulation is rapidly reached. It was shown that the complete consumption of antioxidants coincides with the end of the oxidation induction period and the onset of the sudden decrease in the elongation at break.

Based on all these experimental results, a simplified kinetic model was derived from the main action mechanisms of both types of antioxidants in order to account as faithfully as possible for their consumption kinetics, estimate their antagonistic effects and, using a relevant end-of-life criterion, predict the lifetime of the two XLPE insulations. It was found a satisfying agreement between theory and experiment, which opens interesting research prospects for the evaluation and modeling of the synergistic or antagonistic effects of other usual blends of industrial antioxidants.

AUTHOR CONTRIBUTIONS

Tetiana Salivon: PhD student who undertook the research study in the laboratory. **Rapheal Comte:** Founder and supervisor of the research study. **Xavier Colin:** Supervisor of the research in the laboratory, development of the scientific approach, validation of data for publication and writing of the manuscript.

DATA AVAILABILITY STATEMENT

The data presented in this manuscript are available on request from the corresponding author.

ORCID

Xavier Colin  <https://orcid.org/0000-0001-7768-9000>

REFERENCES

- [1] C. Duval, *Plastiques et Automobile – D'hier à Aujourd'hui*, AM3590, Techniques de l'Ingénieur, Saint-Denis, France **2007**.
- [2] G. Scott, *Atmospheric Oxidation and Antioxidants*, Elsevier Publishing Company, Amsterdam **1965**, p. 66, Ch.3.
- [3] L. Reich, S. S. Stivala, *Autooxidation of Hydrocarbons and Polyolefins*, Marcel Dekker Inc, New-York **1969**, p. 31, Ch.2.
- [4] S. S. Stivala, J. Kimura, S. M. Gabbay, in *Degradation and Stabilisation of Polyolefins* (Ed: N. S. Allen), Applied Science Publishers, London **1983**, p. 63, Ch.3.
- [5] G. Scott, *Atmospheric Oxidation and Antioxidants*, Elsevier Publishing Company, Amsterdam **1965**, p. 115, Ch.4.
- [6] G. Scott, *Atmospheric Oxidation and Antioxidants*, Marcel Dekker Inc, New-York **1965**, p. 170, Ch.5.
- [7] L. Reich, S. S. Stivala, *Autooxidation of Hydrocarbons and Polyolefins*, Marcel Dekker Inc, New-York **1969**, p. 139, Ch.3.
- [8] R. J. Shelton, in *Polymer Stabilization* (Ed: W. L. Hawkins), Wiley-Interscience, New-York **1971**, p. 29, Ch.2.
- [9] Y. Kamiya, E. Niki, in *Aspects of Degradation and Stabilization of Polyolefins* (Ed: H. H. G. Jellinek), Elsevier Scientific Publishing Company, Amsterdam **1978**, p. 79, Ch.3.

- [10] S. Al-Malaika, G. Scott, in *Degradation and Stabilisation of Polyolefins* (Ed: N. S. Allen), Applied Science Publishers, London **1983**, p. 247, Ch.6.
- [11] H. Zweifel, R. D. Maier, M. Schiller, *Plastics Additives Handbook*, 6th ed., Hanser Publishers, Munich **2009**.
- [12] S. Al-Malaika, in *Long Term Properties of Polyolefins* (Ed: A.-C. Albertsson), Springer Berlin Heidelberg, Berlin **2004**, p. 121.
- [13] N. S. Allen, M. Edge, *J. Vinyl Addit. Technol.* **2020**, 27(1), 1.
- [14] X. Colin, B. Fayolle, L. Audouin, J. Verdu, *Polym. Degrad. Stab.* **2003**, 80(1), 67.
- [15] X. Colin, L. Audouin, J. Verdu, *Polym. Degrad. Stab.* **2004**, 86, 309.
- [16] N. Khelidj, X. Colin, L. Audouin, J. Verdu, *Nucl. Instrum. Methods Phys. Res.* **2005**, B236, 88.
- [17] N. Khelidj, X. Colin, L. Audouin, J. Verdu, C. Monchy-Leroy, V. Prunier, *Polym. Degrad. Stab.* **2006**, 91(7), 1593.
- [18] N. Khelidj, X. Colin, L. Audouin, J. Verdu, C. Monchy-Leroy, V. Prunier, *Polym. Degrad. Stab.* **2006**, 91(7), 1598.
- [19] X. Colin, C. Monchy-Leroy, L. Audouin, J. Verdu, *Nucl. Instrum. Methods Phys. Res.* **2007**, 265, 251.
- [20] S. Hettal, S. Roland, K. Sipila, H. Joki, X. Colin, *Polym. Degrad. Stab.* **2021**, 185, 109492.
- [21] S. Hettal, S. V. Suraci, S. Roland, D. Fabiani, X. Colin, *Polymers* **2021**, 13, 4427.
- [22] N. M. Emanuel, A. L. Buchachenko, *Chemical Physics of Polymer Degradation and Stabilization*, VNU Science Press, Utrecht, The Netherlands **1987**, p. 139.
- [23] ISO 6722, *Véhicules Routiers – Câbles Monoconducteurs de 60 V et 600 V – Dimensions, Méthodes d'Essais et Exigences*, Genève **2006**.
- [24] D. M. Dickson Jr., *Stabilized Polyolefin Compositions*, US Patent 3 006 885, Hercules Powder Company, Wilmington **1961**.
- [25] N. P. Neureiter, D. E. Brown, *Ind. Eng. Chem. Prod. Res. Dev.* **1962**, 1, 236.
- [26] W. L. Hawkins, M. A. Worthington, *J. Polym. Sci.: Part A* **1963**, 1(11), 3489.
- [27] G. Scott, *Atmospheric Oxidation and Antioxidants*, Elsevier Publishing Company, Amsterdam **1965**, p. 248, Ch.7.
- [28] C. R. H. I. De Jonge, E. A. Giezen, F. P. B. van der Maeden, W. G. B. Huysmans, W. J. D. Klein, W. J. Mijs, in *Stabilization and Degradation of Polymers. Advances in Chemistry Series No. 169* (Eds: D. L. Allara, W. L. Hawkins), American Chemical Society, Washington **1978**, p. 399, Ch.31.
- [29] C. R. H. I. De Jonge, *Pure Appl. Chem.* **1983**, 55(10), 1637.
- [30] J. Pospisil, in *Oxidation Inhibition in Organic Materials*, Vol. 1 (Eds: J. Pospisil, P. P. Klemchuk), CRC Press, Boca Raton **1990**, p. 173.
- [31] A. Xu, S. Roland, X. Colin, *Polym. Degrad. Stab.* **2020**, 181, 109276.
- [32] A. Xu, S. Roland, X. Colin, *Polym. Degrad. Stab.* **2021**, 183, 109453.
- [33] A. Xu, S. Roland, X. Colin, *Polym. Degrad. Stab.* **2021**, 189, 109597.
- [34] G. Geuskens, M. S. Kabamba, *Polym. Degrad. Stab.* **1982**, 4, 69.
- [35] W. D. Domke, H. Steinke, *J. Polym. Sci., Polym. Chem. Ed.* **1986**, 24, 2701.
- [36] J. Lacoste, D. J. Carlsson, *J. Polym. Sci., Polym. Chem. Ed.* **1992**, 30, 493.
- [37] M. Da Cruz, L. Van Schoors, K. Benzarti, X. Colin, *J. Appl. Polym. Sci.* **2016**, 133(18), 43287.
- [38] G. Rapp, J. Tireau, P.-O. Bussière, J.-M. Chenal, F. Rousset, L. Chazeau, J.-L. Gardette, S. Therias, *Polym. Degrad. Stab.* **2019**, 163, 161.
- [39] C. Blivet, J.-F. Larché, Y. Israeli, P.-O. Bussière, J.-L. Gardette, *Polym. Test.* **2020**, 93, 106913.
- [40] R. G. Bossert, *J. Chem. Ed.* **1950**, 27(1), 10.
- [41] C. Rouillon, *Etude de l'Impact des Vieillissements Photochimique, Thermique et Climatique sur les Propriétés d'Aspect de Polypropylènes Teintés Masse Colorés*, PhD dissertation, Université Blaise Pascal, France **2015**.
- [42] E. G. Palacios, G. Juarez-Lopez, *Hydrometallurgy* **2004**, 72, 139.
- [43] S. Vahur, A. Teearu, P. Peets, L. Joosu, I. Leito, *Anal. Bioanal. Chem.* **2016**, 408, 3373.
- [44] H. L. McMurry, V. Thornton, *Anal. Chem.* **1952**, 24(2), 318.

AUTHOR BIOGRAPHIES

Dr. Tetiana Salivon Former PhD student at Arts et Métiers Institute of Technology and now project manager in the automotive industry.

Mr. Raphael Comte Currently technical referent on the modeling and numerical simulation tools in the field of electricity and electronics at PSA PEUGEOT CITROEN.

Prof. Xavier Colin Currently professor in Materials Chemistry at Arts et Métiers Institute of Technology. Specialist in the aging and durability of polymers and organic composite materials, in particular in the development of kinetic models for lifetime prediction.